PCCP

Cite this: *Phys. Chem. Chem. Phys.*, 2012, **14**, 16618–16625

www.rsc.org/pccp

PAPER

DFT study of coverage-depended adsorption of NH_3 on TiO_2-B (100) surface

Xiao-jing Guo, Weijia Liu, Wei Fang, Lu Cai, Yudan Zhu, Linghong Lu and Xiaohua Lu*

Received 8th April 2012, Accepted 7th August 2012
DOI: 10.1039/c2cp41124e

A previous study showed that TiO_2-B (100) surface is very unique. It is characterised by high activity and a loose structure. In this study, we studied the adsorption of ammonia on TiO_2-B (100) surface at coverages ranging from 1/6 ML to 1 ML using *ab initio* density functional calculations. We also investigated the adsorption of an isolated ammonia molecule on TiO_2-B (001) surface to compare the different activities of TiO_2-B (100) and (001) surfaces towards NH_3. The results showed that the TiO_2-B (100) surface is more reactive towards NH_3 molecule than TiO_2-B (001) surface, and the Lewis acid site on TiO_2-B (100) surface is more acidic. The decrease rate of the average molecular adsorption energy of NH_3 with coverage on TiO_2-B (100) surface is substantially lower than that on a rutile (011) surface above 1/2 ML coverage due to the open structure of TiO_2-B (100) surface. The average molecular adsorption energy shows a linear dependence on the coverage of $y = 111.0 - 36.3x$ on TiO_2-B (100) surface. The possibility of NH_3 molecule onto the Ti_{5c} site is nearly equal to forming a dimer with adsorbed NH_3 on TiO_2-B (100) surface at 5/6 ML coverage.

1. Introduction

Selective catalytic reduction (SCR) of NO_x by NH_3 is one of the most effective ways to control NO_x emission in which ammonia adsorption is the first elementary step.[2–4] As evidenced by many experimental and theoretical studies, ammonia covers the catalyst surface and NO can react from both free and adsorbed states under any catalytic reaction conditions.[2,3] TiO_2 and TiO_2 supported catalysts are most widely used catalysts, and show high activities at low temperature in SCR processes.[5–7] It was reported that the SCR activity increases with the amount of NH_3 chemisorption on TiO_2 surfaces increasing.[5] In some ways, TiO_2 surface with high ammonia adsorption capacity is more suitable for SCR processes. It demands deep understanding of ammonia adsorption on TiO_2 surface under various coverages and seeking TiO_2 surface with high ammonia adsorption strength at high ammonia coverage.

Many efforts for elucidation of ammonia adsorption and coverage effect on ammonia adsorption on TiO_2 surface have been made. Siu *et al.* revealed using Auger-photoelectron coincidence spectroscopy that NH_3 is molecularly adsorbed at every other five-fold coordinated Ti site on rutile (110) surface giving a saturation coverage of half a monolayer.[7] These results were afterwards confirmed by a STM study of Pang *et al.*[8] Through a TPD method, Madix and Farfan-Arribas estimated the desorption activation energy of adsorbed NH_3 on rutile (110) to be 86 kJ mol^{-1}.[9] On the reactive anatase (001) and rutile (011) surfaces, the molecular adsorption mode of NH_3 is confimed favored over the dissociative mode.[10–13] Additionally, it was reported that the dimer formation possibility is related to the saturation coverage of NH_3 molecules on the Pt (100) surface.[14] However, the possibility of ammonia molecules forming a dimer on the TiO_2 surfaces is still unclear.

Though various forms of TiO_2 have the same chemical composition as TiO_2, their crystalline structures are different, resulting in different surface structure arrangements and different surface reactivity with different adsorption abilities. Firstly, the surface reactivity is correlated with the nature and number of coordinatively unsaturated active sites. Vanderbilt and co-workers reported that a higher density of dangling bonds on the surface would result in higher surface energies for rutile TiO_2.[15] Selloni and co-workers remarked that the surface energies for anatase facets almost linearly depend on the density of coordinatively unsaturated Ti cations.[16] We brought a more general criterion for the evaluation of reactivities of different TiO_2 surfaces based on the linkage style of exposed O anions and the ratio of exposed O and Ti atoms.[1] Secondly, the surface structural looseness also affects the surface reactivity and adsorption ability. The structural looseness is related to the charge distribution on the surface and the interaction energy between the adsorbates. Gong and co-workers reported that different interatomic distances on the surface can change the surface reactivity toward adsorption.[17]

State Key Lab of Materials-Oriented Chemical Engineering, Nanjing University of Technology, Xinmofan Road, 5#, Nanjing, Jiangsu Province 210009, China

The results of Tilocca demonstrated that the short distance of adjacent Ti_{5c} sites in the same row could cause significant repulsion between adsorbed water molecules leading to preferential adsorption of further water molecules.[18]

Loose TiO_2 surface could reduce repulsion between adsorbed ammonia molecules leading to high ammonia adsorption strength at high ammonia coverage. Additionally, Vittadini *et al.* pointed out that the structural requirements for SCR catalysts could be the active sites on the surface being rather loose.[19] It seems that TiO_2 materials with a loose surface structure is more suitable for SCR reaction.

TiO_2 occurs in nature as the well-known forms of anatase, rutile and brookite, and additionally as the monoclinic form of TiO_2-B which was afterwards identified to be a naturally occurring form.[20] TiO_2-B is drawing growing attention in its applications of catalysis and photocatalysis.[21–24] Various TiO_2-B nanostructures have been successfully synthesized by several groups.[25–28] Recently, we have synthesized highly crystalline TiO_2-B nanofibers with (100) and (001) facets exposed on the surface using a designed soft chemistry route,[23,29] which show considerable activities in heterogeneous reactions.[24,30,31] We have investigated the adsorption of various small molecules on TiO_2-B surfaces,[1,32,33] and showed that H_2O can dissociate on TiO_2-B (100) surface indicating a very reactive surface.[1] This was confirmed by Vittadini *et al.* with a theoretical approach.[34,35] Additionally, the structure of TiO_2-B (100) surface is very unique and the distance between active five-fold coordinated Ti atoms on TiO_2-B (100) surface is very long as shown in Fig. 1. The fully dissociative adsorption of water at 1 ML coverage on TiO_2-B (100) surface is still favored due to its unique open structure.[1] The high activity and open structure of TiO_2-B (100) surface may in some ways enhance the SCR activity. It is therefore important to understand NH_3 adsorption on TiO_2-B (100) surface with coverage. Related issues include the possibilites of ammonia molecules dissociation and forming a dimer on the surface.

Our current study focuses on the adsorption of NH_3 on TiO_2-B surfaces by means of the density functional theory (DFT) approach to see (1) the different activities of TiO_2-B (100) and (001) surfaces towards NH_3 and (2) the coverage effect on NH_3 adsorption on TiO_2-B (100) surface.

2. Computational model and method

All density functional theory (DFT) calculations were performed using a plane-wave basis set (E_{cut} = 30 Ry) and the generalized gradient approximation (GGA) with the Perdew–Wang 91 (PW91) functional.[36] Ultrasoft pseudopotentials[37] were selected to describe the electron-ion interactions including electrons from H 1s, N and O 2s, 2p and Ti 3s, 3p, 3d and 4s valence shells. All calculations were undertaken with the PWSCF code of Quantum Espresso 4.2.1 package.[38]

The TiO_2-B (100) and (001) surfaces were constructed from the optimized TiO_2-B with parameters reported in our previous study.[1] Periodic slabs of ~10 Å separated by vacuum of 12 Å were used to model TiO_2-B (100) and (001) surfaces. Supercells of $p(3 \times 2)$ and $p(3 \times 1)$ were used for TiO_2-B (100) and (001) surfaces to avoid the interactions of adsorbates from the mirror image, respectively. The dimensions of TiO_2-B (100) and (001) surface supercells are ~13.16 × 11.21 × 22.32 Å and ~11.21 × 12.21 × 22.94 Å. *K*-Point sampling was restricted to the Γ point due to the large dimensions of the supercells. In all calculations, atoms in the bottom half were fixed to their bulk position, while all the rest were free to move. Geometry optimizations were performed until the forces acting on all mobile atoms were below 0.03 eV/Å.

The average molecular adsorption energy was computed according to eqn (1)

$$E_{ave} = (E_s + mE_a - E_{s/ma})/m \quad (1)$$

where E_s, E_a and $E_{a/ma}$ are the energies of the bare surface slab, the isolated NH_3 molecule in the vacuum and the relaxed slab with m NH_3 molecules on the surface; m is the number of adsorbed NH_3 molecules on the surface.

The differential adsorption energy was used to evaluate the adsorption strength of chemisorbed NH_3 when there were one or more NH_3 molecules on the surface. It was calculated as

$$E_{dif} = E_{s/ma} + E_a - E_{s/(m+1)a} \quad (2)$$

where $E_{s/ma}$ ($E_{s/(m+1)a}$) denotes the energy of the system including surface and m (m + 1) monocoordinated NH_3 molecules.

The physically adsorbed NH_3 was also considered in this study. The chemisorbed NH_3 and physically adsorbed one formed a dimer on the surface. The dimer formation energy was calculated according to eqn (3)

$$E_{dim} = E_{s/(n+1)a} + E_a - E_{s/(na+d)} \quad (3)$$

where $E_{s/(n+1)a}$ and $E_{s/(na+d)}$ represent the energies of systems with ammonia molecules monocoordinated to the surface at 1/6 to 5/6 ML coverages and with an ammonia dimer adsorbed on the surface at 1/3 to 1 ML coverages. In the gas phase, they are the energies of an isolated ammonia molecule and the ammonia dimer. We compare the dimer formation energy and the differential adsorption energy to investigate the NH_3 dimer formation possibility on the surface at various coverages.

3. Results and discussion

3.1. Unique structure of TiO_2-B (100) surface

Fig. 1 shows the optimized structures of TiO_2-B (100) and (001), anatase (001) and (101), rutile (011) and (110) surfaces. TiO_2-B (100),[1,34,35] anatase (001)[39–41] and rutile (011)[42,43] surfaces are identified to be reactive with higher surface energies. TiO_2-B (001),[1,35] anatase (101)[16,44] and rutile (110)[16,44,45] are considered to be less reactive with lower surface energies. On the three reactive surfaces, the exposed O_e atoms are exclusively linked to two Ti_e atoms and the ratio of O_e and Ti_e ($R(O_e : Ti_e)$) is equal to 2. In contrast, on the three less reactive TiO_2 surfaces, there are some O_e atoms linking to three Ti_e atoms and $R(O_e : Ti_e)$ = 1.5.

Furthermore, we notice that Ti_e atoms on anatase (001) and rutile (011) surfaces are exclusively five-fold coordinated. Due to the different type of surrounding O atoms, there are two kinds of five-fold coordinated Ti atoms on the surface, denoted as Ti_{5c} and Ti'_{5c}, as shown in Fig. 1. However, there are six-fold coordinated Ti atoms on TiO_2-B (100) surface like anatase (101) and rutile (110) surfaces. The average distance between the active

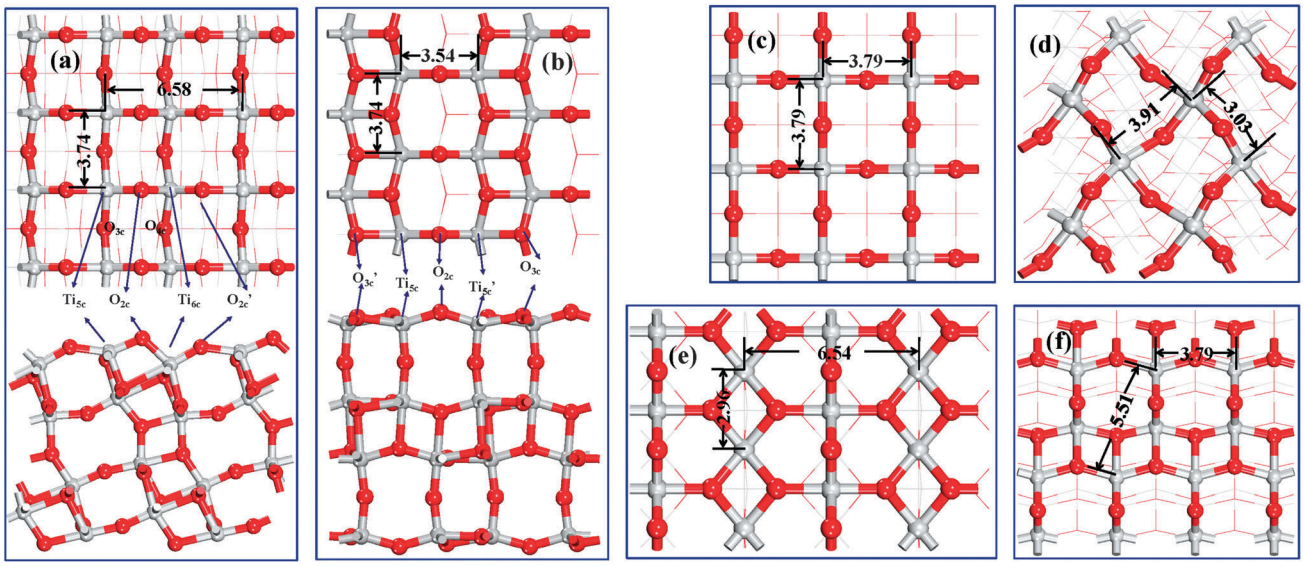

Fig. 1 Geometric models for optimized (a) TiO_2-B (100), (b) TiO_2-B (001), (c) anatase (001), (d) rutile (011), (e) rutile (110) and (f) anatase (101) surfaces. The subscripts of Ti_e and O_e atoms in (a) and (b) denote the coordination numbers on the surface. The coordination numbers of O_{2c}, O'_{2c}, O_{3c} and O'_{3c} in (a) and (b) before the formation of the surface (in bulk) are 3, 2, 4 and 3. The coordination numbers of Ti_{6c}, Ti_{5c} and Ti'_{5c} in (a) and (b) before the formation of the surface (in bulk) are 6. Ti_{5c} in (b) coordinates to two O_{3c} and one O'_{3c}. Ti'_{5c} in (b) coordinates to one O_{3c} and two O'_{3c}. The selected bond distances shown are in Å.

five-fold coordinated Ti atoms on TiO_2-B (100) surface is the longest among all these six TiO_2 surfaces as shown in Fig. 1. In other words, the active adsorption sites on TiO_2-B (100) surface for small molecules are very loose.

3.2. Optimization of NH_3

We first consider the optimization of gas phase NH_3. The supercell approach was employed to avoid lateral interactions between periodic images. The molecule was placed in a large cubic cell with 10 Å side length surrounded by vacuum space. The Brillouin zone was restricted to the gamma point. The obtained values are shown in Table 1. They are in accordance with the experimental values in ref. 46.

3.3. NH_3 adsorption at different coverages

3.3.1. Comparison of adsorption of an isolated NH_3 molecule on TiO_2-B (100) and (001) surfaces (1/6 coverage). NH_3 molecule adsorbs on the surface exclusively through the nitrogen atom of NH_3 to the surface five-fold coordinated titanium atom. Fig. 2 shows the optimized structures for isolated NH_3 molecules on TiO_2-B (100) and (001) surfaces.

After relaxation, a binding energy of 103.7 kJ mol^{-1} is obtained on TiO_2-B (100) surface (Table 2). The symmetry axis of NH_3 molecule is perpendicular to the surface with a Ti–N bond length of 2.238 Å. Due to the interactions between the NH_3 hydrogen atoms and surface two-fold coordinated oxygen atoms, the NH_3 molecule deviates from C_{3v} symmetry slightly with angles ∠ H2–N–H3 and ∠ H1–N–H3 increasing by 3°. The five-fold coordinated titanium atom connecting to NH_3 molecule moves up from the TiO_2-B (100) surface by about 0.007 Å. The neighboring two-fold coordinated oxygen atom moves a little away from the five-fold coordinated titanium atom, resulting in the $Ti_{5c} - O'_{2c}$ bond about 0.040 Å longer than before. In a word, the interaction between the NH_3 nitrogen atom and surface five-fold coordinated titanium atom and the interactions between the NH_3 hydrogen atoms and surface two-fold coordinated oxygen atoms contribute to stabilizing the adsorption structure.

Table 1 Comparison of calculated and observed (ref. 46) geometry of NH_3

Geometry	Cal. (this work)	Exp.[46]
d_{N-H} (Å)	1.023	1.012
H–N–H (degree)	106.5	106.7

There are two kinds of five-fold coordinated titanium atoms, Ti_{5c} and Ti'_{5c}, on TiO_2-B (001) surface. The adsorption energies of NH_3 molecules at Ti_{5c} and Ti'_{5c} sites are 61.5 and 57.1 kJ mol^{-1} respectively (Fig. 2b and c and Table 2). Both are smaller than the adsorption energy of NH_3 on TiO_2-B (100) surface (103.7 kJ mol^{-1}). In accordance with adsorption energies, the bond lengths of N–Ti_{5c} and $N - Ti'_{5c}$ on (001) are 2.321 and 2.337 Å, both longer than N–Ti bonding distance on TiO_2-B (100) surface (2.238 Å).

Fig. 3a shows the DOS of NH_3 molecules before and after adsorption on TiO_2-B (100) and (001) surfaces. We can observe that all the NH_3 states are stabilized upon adsorption. The stabilization degrees follow the order: (100) surface > Ti_{5c} site on (001) surface ≈ Ti'_{5c} site on (001) surface, which is consistent with the order of the adsorption energies. Additionally, the 1e state of NH_3 remains very narrow, whereas the 2a1 and 3a1 states undergo some level of broadening. By comparison, the broadening of the 3a1 state is stronger than that of the 2a1 state. Fig. 3b presents the PDOS of the adsorption systems where only six five-fold coordinated titanium atoms and six two-fold coordinated oxygen atoms exposed on the surface

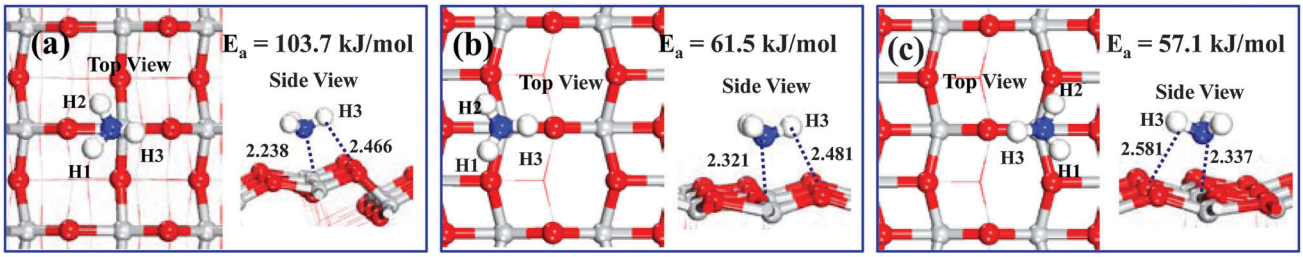

Fig. 2 Configuration of an isolated NH_3 molecule adsorbed (a) on TiO_2-B (100) surface, at (b) Ti_{5c} and (c) Ti'_{5c} sites on TiO_2-B (001) surface. The selected bond distances shown are in Å.

Table 2 Computed structural parameters and adsorption energies of NH_3 molecules on TiO_2-B (100) and (001) surfaces

	TiO_2-B (100) surface, 1/6 ML		TiO_2-B (001) surface, 1/6 ML		
	Mol.[a]	Dis.[b]	Mol.[a] (Ti_{5c})	Mol.[b] (Ti'_{5c})	Dis.[b] (Ti_{5c})
Adsorption energy/kJ mol^{-1}	103.7	61.9	61.5	57.1	−53.1
r(N-Ti)/Å	2.238	1.900	2.321	2.337	1.978
r(N-H1)/Å	1.023	1.020	1.022	1.021	1.020
r(N-H2)/Å	1.023	1.020	1.022	1.022	1.020
r(N-H3)/Å	1.024		1.022	1.022	
r(O-H3)/Å	2.466	0.972	2.481	2.581	0.998
Figure	Fig. 2a	Fig. 5b	Fig. 2b	Fig. 2c	Fig. 5c

[a] Mol. represents the molecular adsorption of NH_3. [b] Dis. represents the dissociative adsorption of NH_3.

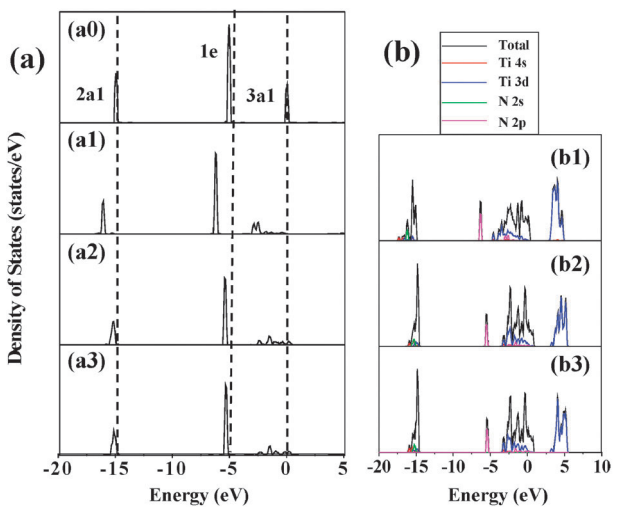

Fig. 3 (a): DOS of an isolated NH_3 molecule (a0) in the gas phase, (a1) on TiO_2-B (100), at (a2) Ti_{5c} and (a3) Ti'_{5c} sites on TiO_2-B (001) surface. (b): projected density of states of adsorption configurations in (b1) Fig. 2a, (b2) Fig. 2b and (b3) Fig. 2c.

are displayed. We can conclude that the N 2s and 2p states of NH_3 molecule mainly contribute to the 2a1 and 1e states. Specifically, the scattering of the NH_3 3a1 (2a1) state is due to the interaction between N 2p (2s) state and Ti 3d (4s, 3d) state. The PDOS results demonstrate that the bonding of the NH_3 molecule to the surface mainly arises from the mixing of the N 2s, 2p and Ti 4s, 3d states.

Fig. 4 shows the density difference planes perpendicular to TiO_2-B (100) and (001) surfaces passing through the N atoms of NH_3 molecules. For all the adsorption structures, the main electron rearrangement takes place along the Ti_{5c} (Ti'_{5c})–N bond. Additionally, the neighboring surface O atoms contribute to stabilizing the molecule. Stronger accumulation of electron density can be found between the molecule and TiO_2-B (100) surface than between the molecule and TiO_2-B (001) surface in accordance with the adsorption energy and DOS analysis. The variation pattern of electron density is in line with the common understanding that the NH_3–TiO_2 interaction is due to the NH_3 molecule donating a lone pair to the TiO_2 surface orbitals.[47]

Fig. 5 presents the Bader atomic charges for free and adsorbed NH_3 on TiO_2-B (100) and (001) surfaces. As observed from Fig. 5, the NH_3 molecule acts as an electron donor for TiO_2-B (100) surface with part of the exceeding electron (0.13 e) diffusing from NH_3 molecule to the surface. Similarly, the net

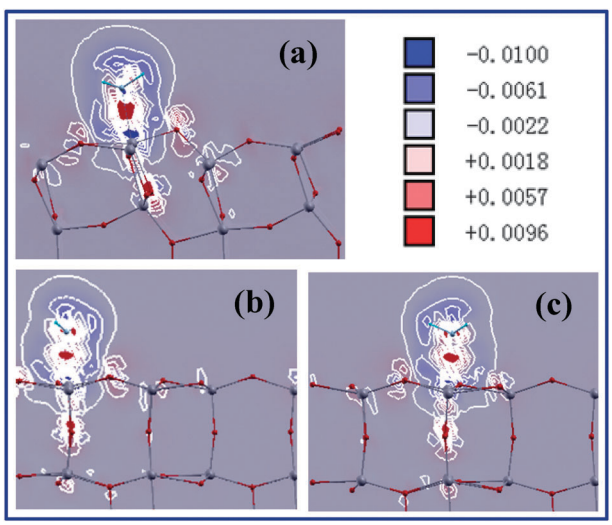

Fig. 4 Electron density difference plots for cuts perpendicular to the surfaces passing through the nitrogen atoms of adsorbed NH_3 molecules (a) on TiO_2-B (100), at (b) Ti_{5c} and (c) Ti'_{5c} sites on TiO_2-B (001) surface.

NH_3 molecules donate 0.10 e and 0.09 e electrons to TiO_2-B (001) surface when the adsorptions take place at Ti_{5c} and Ti'_{5c} sites on (001) surface. These results are consistent with the findings of Chang.[48] They also found NH_3 molecules act as electron donors.[48] In other words, TiO_2-B (100) surface can accept more electrons from NH_3 molecule than (001) surface.

We also investigate the dissociative adsorption of NH_3 on the two surfaces. Upon dissociation, the NH_3 molecule loses a hydrogen atom to one nearby O_{2c} atom by breaking a N–H bond as shown in Fig. 6. On TiO_2-B (100) surface, the one shown in Fig. 6(a) is 20.6 kJ mol^{-1} less stable than the one in Fig. 6(b). The latter is more popular because it decreases the attractive interaction between the NH_2 and H fragments. The larger the attractive interaction is, the more inclined the fragments from NH_3 molecule. The calculated interaction energies between the NH_2 and H fragments are 84.1 kJ mol^{-1} and 8.3 kJ mol^{-1} in Fig. 6(a) and (b), respectively. We found the dissociative process is strongly endothermic on TiO_2-B (001) surface and did not discuss it further. Through the calculated adsorption energies, we can conclude that the molecular adsorption mode is much more favorable than the dissociative adsorption mode for NH_3 on TiO_2-B (100) and (001) surfaces, as reported also on other TiO_2 surfaces.[10–12]

3.3.2. Adsorption of two NH_3 molecules (1/3 ML coverage).

Addition of a second NH_3 molecule to the surface, the NH_3–NH_3 interaction competes with the TiO_2–NH_3 interaction. As presented in Fig. 7, the most stable is a single NH_3 molecule connecting to the surface Ti_{5c} atom in a configuration similar to that of an isolated molecule adsorption (2M1). The calculated average adsorption energy is 99.9 kJ mol^{-1}, very similar to the adsorption energy at 1/6 ML coverage. Consistent with this, the adsorption structures of NH_3 molecules are similar to that at 1/6 coverage with two Ti_{5c}–N bonds of 2.251 and 2.246 Å, drawing up both Ti_{5c} sites by about 0.007 Å. According to the definition, the differential binding energy is the energy gap between the systems with one and two NH_3 molecules on the surface. It turns out to be 95.9 kJ mol^{-1}. Rotation of the NH_3 molecules to different orientations as 2M2 and 2M3 shown in Fig. 7 both produce average adsorption energies of 99.7 kJ mol^{-1}, almost the same as 2M1.

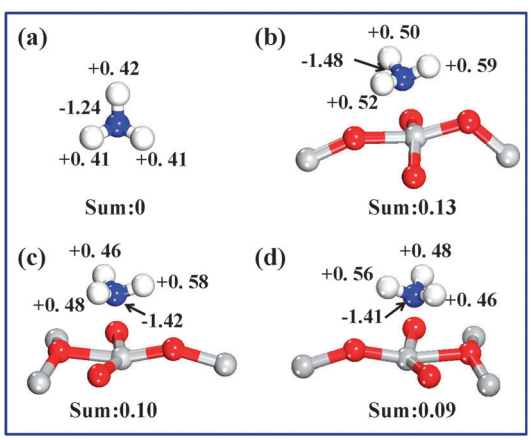

Fig. 5 Bader atomic charge analysis of the NH_3 molecule and NH_3 adsorbed onto TiO_2-B surfaces, (a) NH_3, (b) NH_3 on TiO_2-B (100) surface, (c) NH_3 at Ti_{5c} sites on TiO_2-B (001) surface, (d) NH_3 at Ti'_{5c} sites on TiO_2-B (001) surface.

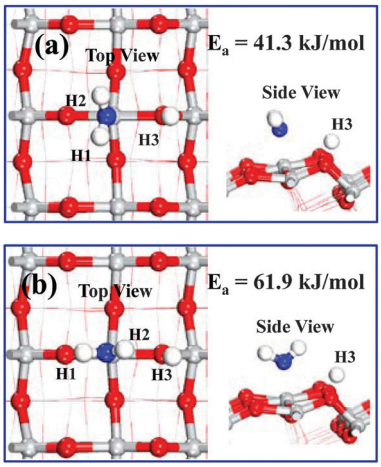

Fig. 6 Dissociative adsorption configurations of an isolated NH_3 molecule on TiO_2-B (100) surface.

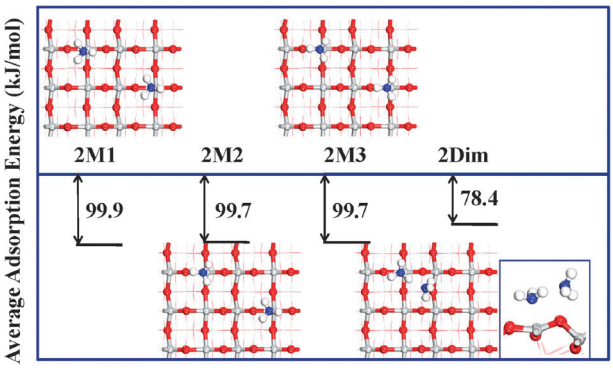

Fig. 7 Molecular and dimeric adsorption configurations of NH_3 at 1/3 ML coverage on TiO_2-B (100) surface. Inset is the side view of the NH_3 dimer. The unit of the average adsorption energy is kJ mol^{-1}.

Besides these adsorption structures, we also find a stable configuration in which the two NH_3 molecules form a dimer with an average adsorption energy of 78.4 kJ mol^{-1}. The first molecule binds to the surface through an ammonia N atom to the surface Ti_{5c} atom. The second molecule is hydrogen-bonded *via* its N atom to one H atom of the first molecule (2Dim). The Ti_{5c}–N bond is 2.189 Å, by 0.049 Å shorter than that of an isolated molecule adsorption. The dimer formation energy is 56.4 kJ mol^{-1}, which is about 42.1 kJ mol^{-1} larger than that in the gas phase (Table 3). Consistent with this, the length of the hydrogen bond of the dimer decreases from 2.217 Å in the gas phase to 1.839 Å on TiO_2-B (100) surface. The first molecule donates electrons to the surface leaving the molecule positively charged. The second molecule acts as a lone pair donor to the first molecule, and this allows stronger interaction between the first molecule and the surface.

3.3.3. Adsorption of three NH_3 molecules (1/2 ML coverage).

Different adsorption configurations of three NH_3 molecules (1/2 ML coverage) on TiO_2-B (100) surface are shown in Fig. 8. The most favorable one (3M1) is with an average adsorption energy of 93.5 kJ mol^{-1}, 10.2 kJ mol^{-1} and 6.4 kJ mol^{-1}

Table 3 Computed dimer formation energies and N–H bond length of the dimer in the gas phase (in this work and ref. 14) and as a function of coverage on TiO_2-B (100) surface

	Gas		TiO_2-B (100)				
			1/3 ML	1/2 ML	2/3 ML	5/6 ML	1 ML
E_{df}[a] (kJ mol^{-1})	14.4	14.5[14]	56.4	53.6	53.2	52.0	51.5
d_{N-H}[b] (Å)	2.217	2.390[14]	1.839	1.852	1.855	1.862	1.869

[a] E_{df} is the computed dimer formation energy. [b] d_{N-H} is the calculated N–H bond length of the dimer.

smaller than those at 1/6 and 1/3 coverages. The Ti_{5c}–N(A) and Ti_{5c}–N(B) bonds are with a nearly equal length of about 2.270 Å, and the Ti_{5c}–N(C) bond is a bit shorter with 2.253 Å. The differential binding energy at this coverage is 80.5 kJ mol^{-1}. Competing with this are 3M2, 3M3 and 3M4 in Fig. 7 with similar binding energies of 93.4, 93.2 and 91.7 kJ mol^{-1}. 3M1 decreases, to some extent, the lateral repulsion between molecules A and B compare to 3M2 and 3M3. Additionally, the repulsive interaction between molecules A and C is the largest in 3M4. This makes 3M1 the most favorable, and 3M4 the most unfavorable configuration.

The most stable dimeric adsorption of NH_3 (the dimeric adsorptions of NH_3 in this work stands for an ammonia dimer and 0 to 4 NH_3 molecules on the surface at 1/3 to 1 ML coverages.) at 1/2 ML coverage (3Dim) turns out to be with an average adsorption energy of 83.8 kJ mol^{-1}. It is by 9.7 kJ mol^{-1} less stable than 3M1, but by 5.3 kJ mol^{-1} more stable than the dimeric adsorption of NH_3 at 1/3 ML coverage (2Dim). Two NH_3 molecules respectively bind to the surface Ti_{5c} atoms, and the third one is hydrogen-bonded to one of the first two adsorbates forming a dimer. The dimer formation energy in this case is 53.6 kJ mol^{-1} (Table 3), only 2. 8 kJ mol^{-1} smaller than that at 1/3 ML coverage. The hydrogen bond of the dimer turns out to be 1.852 Å, 0.013 Å longer than that at 1/3 ML coverage.

3.3.4. Adsorption of four/five/six NH_3 molecules (2/3 ML, 5/6 ML, 1 ML coverages). Six adsorbates saturate the surface cationic sites. Increasing the number of adsorbates to four, five and six will result in large lateral repulsion. 4 M, 5 M and 6 M are the most favorable molecular adsorption structures shown in Fig. 9 as a compromise of the intermolecular force among NH_3 molecules and the force between the surface and NH_3 molecules. The adsorption energies decrease to 87.2, 80.3 and 74.4 kJ mol^{-1} at 2/3 ML, 5/6 ML and 1 ML NH_3 coverages, respectively, due to lateral repulsion. The differential binding energies turn out to be 74.4, 52.7 and 44.7 kJ mol^{-1} at 2/3 ML, 5/6 ML and 1 ML NH_3 coverages, respectively.

We find the dimeric adsorptions of NH_3 3.8 kJ mol^{-1} less stable than, of comparative stability with, and 1.8 kJ mol^{-1} more favorable than, the molecular adsorption cases of NH_3 molecules monocoordinated to the surface at 2/3 ML, 5/6 ML and 1 ML coverages (4Dim, 5Dim and 6Dim). The dimer formation energies are 53.2, 52.0 and 51.5 kJ mol^{-1} at these three coverages (Table 3). The hydrogen bond lengths of the dimers are 1.855, 1.862 and 1.869 Å in 4Dim, 5Dim and 6Dim. The dimer formation energy is smaller, comparative to and larger than the differential binding energy at 2/3 ML, 5/6 ML and 1 ML NH_3 coverages, respectively.

3.4. Coverage effects on NH_3 adsorption on TiO_2-B (100) surface

Furthermore, we discuss the energetic trend as a function of NH_3 coverage on TiO_2-B (100) surface. Fig. 10 presents the average molecular adsorption energy, the differential binding energy and dimer formation energy in the optimal geometries at different coverages. The average molecular adsorption energy shows a linear dependence on the coverage. A corresponding linear fit ($y = 111.0 - 36.3x$) is also shown in Fig. 10. We should notice that the average molecular adsorption energy decrease rate from 1/2 ML to 1 ML coverage on TiO_2-B (100) surface is 20.4% ((93.5–74.4)/93.5). However, the average molecular adsorption energy decrease rate of NH_3 on rutile (011) surface, from 1/2 ML to 1 ML coverage is about 42.0% presented in the study of McGill *et al.*[11] We believe the smaller decrease rate of the average molecular adsorption energy at higher coverage on TiO_2-B (100) compared to rutile (011) surfaces is related to the unique open structure of TiO_2-B (100) surface. The differential binding energy decreases in magnitude monotonously along with the coverage increasing. The differential binding energy at 1/3 ML is more than twice that at 1 ML coverage. By contrast, the decline of dimer formation energy is very small with ammonia coverage. The dimer formation energy gap is only 4.9 kJ mol^{-1} between the largest and the smallest values. The dimer

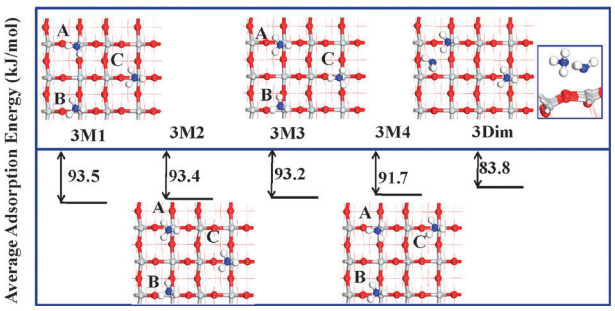

Fig. 8 Molecular and dimeric adsorption configurations of NH_3 at 1/2 ML coverage on TiO_2-B (100) surface. Inset is a side view of the NH_3 dimer. The unit of the average adsorption energy is kJ mol^{-1}.

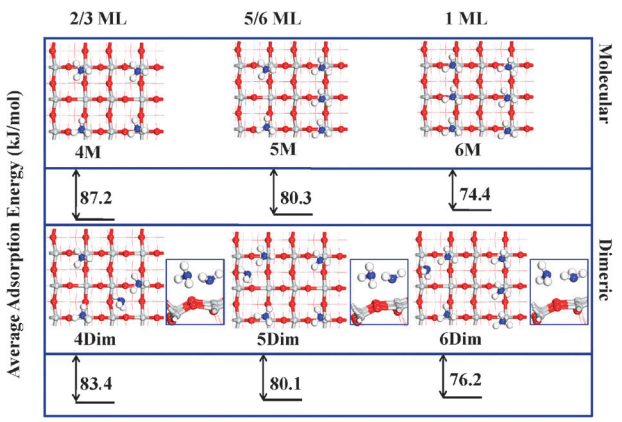

Fig. 9 Molecular and dimeric adsorption configurations of NH_3 at 2/3 ML, 5/6 ML and 1 ML coverages on TiO_2-B (100) surface. Inset is the side view of the NH_3 dimer. The unit of the average adsorption energy is kJ mol^{-1}.

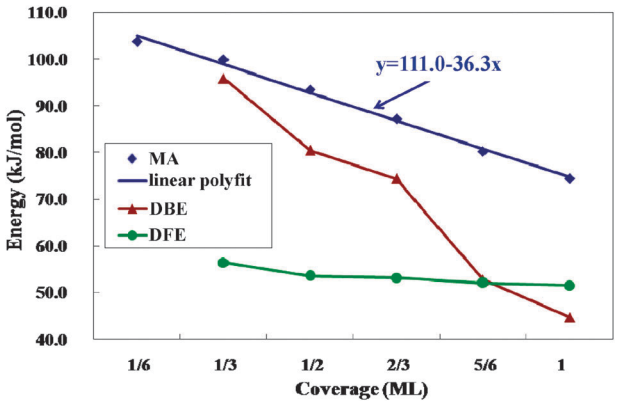

Fig. 10 Average molecular adsorption energy (MA), differential binding energy (DBE) and dimer formation energy (DFE) of NH_3 molecule as a function of coverage on TiO_2-B (100) surface.

formation energy is smaller than the differential binding energy at coverages below 2/3 ML, but comparative to and larger than the differential binding energy at 5/6 and 1 ML NH_3 coverages. This means that the possibility of the fifth NH_3 molecule onto the Ti_{5c} site is nearly equal to that forming a dimer with adsorbed NH_3 when there are four NH_3 molecules monocoordinated to Ti_{5c} atoms on TiO_2-B (100) surface. Cortés Bracho *et al.* reported that the relative magnitude of dimer formation energy and differential binding energy is related to the saturation coverage of NH_3 molecules on the Pt (100) surface.[14] This is related to the possible adsorption amount of NH_3 on TiO_2-B (100) surface which is important in SCR and SCO reactions. As for this point, maybe TiO_2-B with a reactive (100) facet on the surface is possibly more suitable for SCR, SCO reactions.

4. Conclusions

In this work, we presented a comprehensive DFT investigation of the ammonia adsorption at coverages ranging from 1/6 to 1 ML on the unique TiO_2-B (100) surface. The ammonia adsorption energy on TiO_2-B (100) surface is larger than that on TiO_2-B (001) surface indicating that the TiO_2-B (100) surface is more reactive towards NH_3 than TiO_2-B (001) surface. TiO_2-B (100) surface can accept more electrons from NH_3 molecule than (001) surface resulting in a stronger Lewis acid site on TiO_2-B (100) surface. The average molecular adsorption energy shows a linear dependence on the coverage of $y = 111.0 - 36.3x$. Due to its unique open structure, the decrease rate of the average molecular adsorption energy of ammonia on TiO_2-B (100) surface is far smaller than that on rutile (011) surface. Although the differential binding energy decreases strongly with the coverage increasing, the dimer formation energy decreases only slightly with ammonia coverage. The possibility of the fifth NH_3 molecule monocoordinating to the Ti_{5c} site is nearly equal to that forming a dimer with adsorbed NH_3 at 5/6 ML coverage.

Acknowledgements

This work was supported by the Program for Changjiang Scholars and Innovative Research Team in University (PCSIRT 0732), the National Natural Science Foundation of China Grants (No. 21136004, 20736002, 21176113 and 20876073), NSFC-RGC (No. 20731160614) and National Basic Research Program of China (No. 2009CB623407, 2009CB219902 and 2009CB226103). The authors also acknowledge financial support from the Jiangsu Applied Chemistry and Materials Graduate Center for Innovation and the Academic Communication Foundation (No. 2010ACMC03) and the China Postdoctoral Science Foundation (20110491407).

References

1 W. J. Liu, J. G. Wang, W. Li, X. J. Guo, L. H. Lu, X. H. Lu, X. Feng, C. Liu and Z. H. Yang, *Phys. Chem. Chem. Phys.*, 2010, **12**, 8721–8727.
2 N. U. Zhanpeisov, S. Higashimoto and M. Anpo, *Int. J. Quantum Chem.*, 2001, **84**, 677–685.
3 G. Ramis, G. Busca and V. Lorenzelli, *Appl. Catal.*, 1990, **64**, 243–257.
4 G. Busca, L. Lietti, G. Ramis and F. Berti, *Appl. Catal., B*, 1998, **18**, 1–36.
5 S. Yamazoe, T. Okumura, K. Teramura and T. Tanaka, *Catal. Today*, 2006, **111**, 266–270.
6 R. Jin, Y. Liu, Z. Wu, H. Wang and T. Gu, *Chemosphere*, 2010, **78**, 1160–1166.
7 W. K. Siu, R. A. Bartynski and S. L. Hulbert, *J. Chem. Phys.*, 2000, **113**, 10697–10702.
8 C. L. Pang, A. Sasahara and H. Onishi, *Nanotechnology*, 2007, **18**, 044003.
9 E. Farfan-Arribas and R. J. Madix, *J. Phys. Chem. B*, 2003, **107**, 3225–3233.
10 I. Onal, S. Soyer and S. Senkan, *Surf. Sci.*, 2006, **600**, 2457–2469.
11 P. R. McGill and H. Idriss, *Langmuir*, 2008, **24**, 97–104.
12 R. Erdogan, O. Ozbek and I. Onal, *Surf. Sci.*, 2010, **604**, 1029–1033.
13 J. N. Wilson and H. Idriss, *Langmuir*, 2004, **20**, 10956–10961.
14 O. L. Cortés Bracho, V. A. Ranea, I. M. Irurzun, R. Imbihl and E. E. Mola, *Chem. Phys. Lett.*, 2011, **505**, 21–25.
15 M. Ramamoorthy, D. Vanderbilt and R. D. King-Smith, *Phys. Rev. B: Condens. Matter*, 1994, **49**, 16721–16727.
16 M. Lazzeri, A. Vittadini and A. Selloni, *Phys. Rev. B: Condens. Matter*, 2001, **63**, 155409.
17 W.-K. Li, X.-Q. Gong, G. Lu and A. Selloni, *J. Phys. Chem. C*, 2008, **112**, 6594–6596.
18 Y. He, A. Tilocca, O. Dulub, A. Selloni and U. Diebold, *Nat. Mater.*, 2009, **8**, 585–589.
19 A. Vittadini, M. Casarin and A. Selloni, *J. Phys. Chem. B*, 2005, **109**, 1652–1655.
20 J. F. Banfield, D. R. Veblen and D. J. Smith, *Am. Mineral.*, 1991, **76**, 343–353.
21 J. Zhu, J. Zhang, F. Chen, K. Iino and M. Anpo, *Top. Catal.*, 2005, **35**, 261–268.
22 X. Zhang, J. H. Pan, A. J. Du, P. F. Lee, D. D. Sun and J. O. Leckie, *Chem. Lett.*, 2008, **37**, 424–425.
23 W. Li, C. Liu, Y. Zhou, Y. Bai, X. Feng, Z. Yang, L. Lu, X. Lu and K.-Y. Chan, *J. Phys. Chem. C*, 2008, **112**, 20539–20545.
24 Y. Bai, W. Li, C. Liu, Z. Yang, X. Feng, X. Lu and K.-Y. Chan, *J. Mater. Chem.*, 2009, **19**, 7055–7061.
25 M. Kobayashi, V. V. Petrykin, M. Kakihana, K. Tomita and M. Yoshimura, *Chem. Mater.*, 2007, **19**, 5373–5376.
26 W. A. Daoud and G. K. H. Pang, *J. Phys. Chem. B*, 2006, **110**, 25746–25750.
27 G. Armstrong, A. R. Armstrong, J. Canales and P. G. Bruce, *Chem. Commun.*, 2005, 2454–2456.
28 A. R. Armstrong, G. Armstrong, J. Canales and P. G. Bruce, *Angew. Chem., Int. Ed.*, 2004, **43**, 2286–2288.
29 M. He, X.-H. Lu, X. Feng, L. Yu and Z.-H. Yang, *Chem. Commun.*, 2004, 2202–2203.
30 Y. Bai, Y. Zhang, W. Li, X. Zhou, C. Wang, X. Feng, L. Zhang and X. Lu, *Appl. Surf. Sci.*, 2009, **255**, 9296–9300.
31 W. Li, Y. Bai, C. Liu, Z. Yang, X. Feng, X. Lu, N. K. van der Laak and K.-Y. Chan, *Environ. Sci. Technol.*, 2009, **43**, 5423–5428.

32 W. J. Liu, J. G. Wang, X. J. Guo, W. Fang, M. J. Wei, X. H. Lu and L. H. Lu, *Catal. Today*, 2011, **165**, 32–40.
33 W. Fang, W. J. Liu, X. J. Guo, X. H. Lu and L. H. Lu, *J. Phys. Chem. C*, 2011, **115**, 8622–8629.
34 A. Vittadini, M. Casarin and A. Selloni, *J. Mater. Chem.*, 2010, **20**, 5871–5877.
35 A. Vittadini, M. Casarin and A. Selloni, *J. Phys. Chem. C*, 2009, **113**, 18973–18977.
36 J. P. Perdew, J. A. Chevary, S. H. Vosko, K. A. Jackson, M. R. Pederson, D. J. Singh and C. Fiolhais, *Phys. Rev. B: Condens. Matter*, 1992, **46**, 6671–6687.
37 D. Vanderbilt, *Phys. Rev. B: Condens. Matter*, 1990, **41**, 7892–7895.
38 G. Paolo, B. Stefano, B. Nicola, C. Matteo, C. Roberto, C. Carlo, C. Davide, L. C. Guido, C. Matteo, D. Ismaila, C. Andrea Dal, G. Stefano de, F. Stefano, F. Guido, G. Ralph, G. Uwe, G. Christos, K. Anton, L. Michele, M.-S. Layla, M. Nicola, M. Francesco, M. Riccardo, P. Stefano, P. Alfredo, P. Lorenzo, S. Carlo, S. Sandro, S. Gabriele, P. S. Ari, S. Alexander, U. Paolo and M. W. Renata, *J. Phys.: Condens. Matter*, 2009, **21**, 395502.
39 X.-Q. Gong and A. Selloni, *J. Phys. Chem. B*, 2005, **109**, 19560–19562.
40 A. Selloni, *Nat. Mater.*, 2008, **7**, 613–615.
41 H. G. Yang, C. H. Sun, S. Z. Qiao, J. Zou, G. Liu, S. C. Smith, H. M. Cheng and G. Q. Lu, *Nature*, 2008, **453**, 638–641.
42 C. Di Valentin, A. Tilocca, A. Selloni, T. J. Beck, A. Klust, M. Batzill, Y. Losovyj and U. Diebold, *J. Am. Chem. Soc.*, 2005, **127**, 9895–9903.
43 T. Kubo, H. Orita and H. Nozoye, *J. Am. Chem. Soc.*, 2007, **129**, 10474–10478.
44 M. Lazzeri, A. Vittadini and A. Selloni, *Phys. Rev. B: Condens. Matter*, 2002, **65**, 119901.
45 A. Kiejna, *et al.*, *J. Phys.: Condens. Matter*, 2006, **18**, 4207.
46 C. R. Company, *Handbook of chemistry and physics*, Chemical Rubber Pub. Co., 1964.
47 G. Ertl, H. Knözinger and J. Weitkamp, *Handbook of heterogeneous catalysis*, VCH, 1997.
48 J.-G. Chang, H.-T. Chen, S.-P. Ju, H.-L. Chen and C.-C. Hwang, *Langmuir*, 2010, **26**, 4813–4821.